

## Study On Improvement Water Deposition on Vehicle Side Mirror

Amirul Syahmi Azhar<sup>1</sup>, Rahmah Mahmudin<sup>1\*</sup>

<sup>1</sup>Department of Mechanical Engineering Technology, Faculty of Engineering Technology,  
Universiti Tun Hussein Onn Malaysia, 84600 Panchor, Johor, MALAYSIA

\*Corresponding Author Designation

DOI: <https://doi.org/10.30880/peat.2023.04.02.059>

Received 02 July 2023; Accepted 12 July 2023; Available online 12 July 2023

**Abstract:** Vehicle side mirror contributes to enable the driver to see the back of the car when parking or driving down the road. The air turbulence caused by passing through the side mirror's neck will cause a raindrop to cover the car's front door mirror. Additionally, Malaysia has a tropical climate, which means that it frequently has rainy days. This situation will result in water deposition near door windows mirror, especially in the front area. The objective of this study is to minimize water deposition on the side mirror. Additionally, one of the major goals of this study is to evaluate the model's simulation using ANSYS software. To prepare for this research, a model must be scanned by a 3D scanner, with the shark fin features will add using the SolidWorks software, and the simulation ran using the ANSYS software. To execute a test with specific conditions for the new model, the boundary condition will be specified towards it in the ANSYS software. Based on finding that been get, the model without any additional shark fin has a better result of turbulence kinetic energy but has worst result on side mirror. For the model with additional shark fin has a little bit improvement at side mirror. Therefore, it can be concluded that the addition of a shark fin, particularly at the base of the side mirror, can contribute to the reduction of turbulence kinetic energy and improve aerodynamic performance in terms of water deposition. To enhance the quality of data in future research, several recommendations can be proposed. Firstly, during the meshing process in the ANSYS simulation, it is advisable to employ a more detailed meshing technique.

**Keywords:** Side mirror, Aerodynamic, Computational Fluid Dynamics CFD

### 1. Introduction

Vehicle aerodynamics are one of the factors that can affect water deposition happening on the vehicle [1]. The primary objective of the research is to identify if the modification can improve water deposition on vehicle side mirrors. Water deposition happening because of airflow that act on the vehicle. The side mirror found in cars, especially in high mass recreational and commercial vehicles,

are water deposition because of a variety of things such the mirror's huge size, the wind, and the heaviness of rain during rainy day [2].

Unsteady vehicle aerodynamic effects have a significant impact on the deposition of water and solid pollutants on car surfaces. The reason for water deposition happening is because airborne water droplets that are lifted as spray by tires or fall as rain combine with wakes, vortices, and shear flows to build up on vehicle surfaces. The management of surface water over the front side glass and the deposition of pollutants on the rear surfaces are given particular attention since the same aerodynamic processes also influence the movement of surface water droplets, rivulets, and films [3]. Due to droplet impact, or "splash," on the mirror surface and the ensuing droplet break-up and rebound, the local water in the side screen may grow [4]. Water that is dropped by droplet "splash" or "spread" regimes on the mirror housing runs over the surface and gathers at the back of the housing. Then, within the aftermath of the mirror, the dirt/water mixture may be dispersed as droplets. The mirror wake direction affects the path that discharged droplets take. That is how the water deposition happens on any vehicle surface.

The problem during heavy weather or rainy day, the driver visibility on the road will interrupt by the raindrop that stick to the side mirror or windshield. As the view of the driver passes through the raindrop, the field of view refracted by a spherical drop is about  $165^\circ$  and assimilates the drop with a fish-eye lens [5]. The water deposition that acts on the side mirror can be affected because of the side mirror position or shape and it can make the water deposition of that vehicle worse or not. Usually, the side mirror position has 2 common positions or more specifically has 2 bases, the first one is horizontal base and the other is angular base [6]. Both locations will give different outcomes of aerodynamic effect and visibility for the driver. The poorly designed side mirror can greatly increase the water deposition on it. Since the modification and optimizing the performance of side mirror is difficult and may take a lot of time, additional bionic shark fin on side mirror is another good option [7].

## 2. Methodology

The approach, simulation, setting, strategy, and mathematical formula are all mentioned in this study. In this study, data is gathered and computational fluid analysis is carried out using the ANSYS FLUENT software. In order to accomplish the research's goal and produce the best possible findings, the study's boundaries and restrictions are crucial. The study's findings used earlier research as a model for conducting current investigation.

A side mirror with various parameters is the geometry design employed in this study to execute the experiment. The simulation is then launched by setting up the parameter in Ansys Fluent. Mesh sizes are established with the appropriate size before moving on to the next phase to ensure the outcome data are valid. The simulation is then started and used to perform the calculation. Following that, the outcome is obtained, and the software can be used to view the airflow pattern and auditory contour.

### 2.1 Model Design

In this research, there have been three types of side mirror that have been through simulation. In Figure 1 shows design without additional shark fin, in Figure 2 is design with additional shark fin side mirror and in Figure 3 is the design with additional shark fin at side mirror [8]. The side mirror has been modified by using Solidworks software.

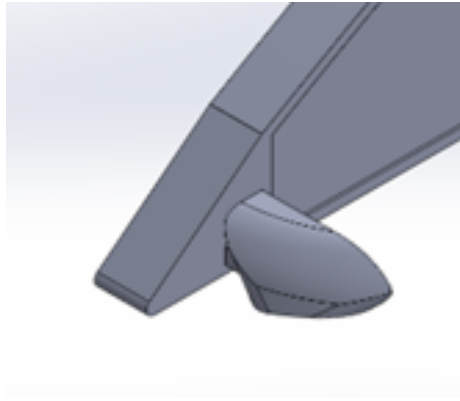


**Figure 1: Side Mirror without Additional Shark Fin**

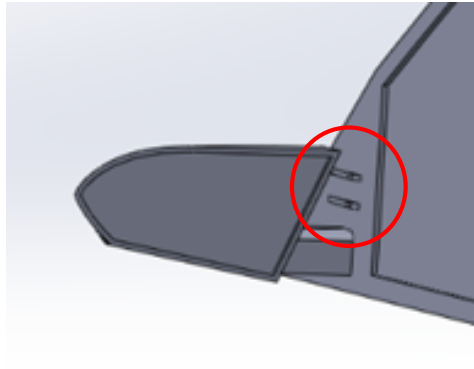


**Figure 2: Side Mirror with Additional Shark Fin at Base**

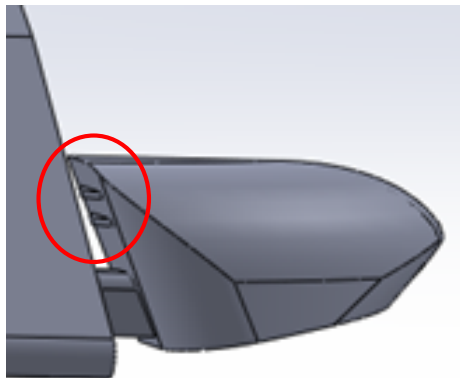


**Figure 3: Side Mirror with Additional Shark Fin**

## 2.2 Geometry Model

In the current optimization study, an enclosed computational domain was created to model how the air flow was dispersed over the mirror. Figure 4 below shows the computational region where the air flow simulation process is carried out. The computational volume has a 0.1 m width, 0.1 m height, and 0.1 m length. In this optimization analysis, the air flow on the stationary mirror model is simulated together with the fluid flow.

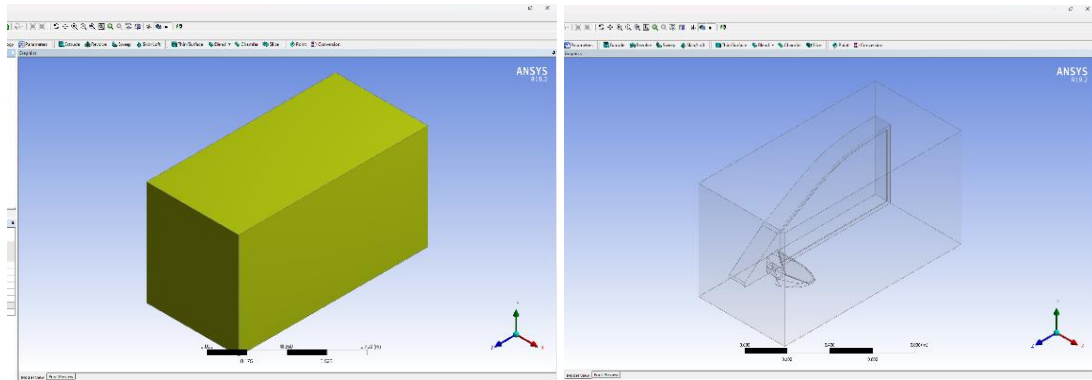


**Figure 4: Enclosure and Boolean on the simulation model**

### 2.3 Meshing

Meshing can be defined as the process of dividing the entire component into number of elements when the load is applied to the model, the load is uniformly distributed as meshing. The accuracy of quality of the meshing can be done by set the meshing parameter to the smaller surface. During meshing process, the position of inlet, outlet and the wall will be determined.

**Table 1: Meshing Setting**

<i>Display</i>	
<i>Display Style</i>	<i>Use Geometry Setting</i>
<i>Defaults</i>	
<i>Physics Preference</i>	<i>CFD</i>
<i>Solver Preference</i>	<i>Fluent</i>
<i>Element Order</i>	<i>Linear</i>
<i>Element Size</i>	<i>Default (7.2841e-002m)</i>
<i>Export Format</i>	<i>Standard</i>
<i>Export Preview Surface Mesh</i>	<i>No</i>
<i>Sizing</i>	
<i>Use Adaptive Sizing</i>	<i>No</i>
<i>Growth Size</i>	<i>1.2</i>
<i>Max size</i>	<i>0.14568m</i>
<i>Mesh Defeaturing</i>	<i>Yes</i>
<i>Defeaturing Size</i>	<i>Default (3.642e-004m)</i>
<i>Capture Curvature</i>	<i>Yes</i>
<i>Curvature Min Size</i>	<i>Default (7.2841e-004m)</i>
<i>Quality</i>	
<i>Check Quality Mesh</i>	<i>Yes, Error</i>
<i>Smoothing</i>	<i>High</i>
<i>Inflation</i>	
<i>Use Automatic Inflation</i>	<i>None</i>
<i>Inflation Option</i>	<i>Smooth Transition</i>
<i>First Aspect Ratio</i>	<i>5</i>
<i>Growth Rate</i>	<i>1.2</i>
<i>Statistics</i>	
<i>Elements</i>	<i>70015</i>
<i>Nodes</i>	<i>13302</i>
<i>Mesh Metric</i>	<i>None</i>

### 2.4 Setup

A velocity in inlet will be set by three different velocity (50km/h, 60km/h, and 70km/h). This will be used to determine the value of turbulence kinetic energy and streamline behavior that act on the side mirror model.

**Table 2: Detail Parameter**

Parameter	Description
Velocity Inlet	50km/h, 60km/h, and 70km/h
<b>Model</b>	
Viscous	K-epsilon
<b>Material</b>	
Fluid	Air
Solid	Aluminum
<b>Method</b>	
Scheme	Couple
Gradient	Least Square Cell Based
Pressure	Second Order
Momentum	Second Order Upwind
Turbulence Kinetic energy	First Order Upwind
Turbulence Dissipation Rate	First Order Upwind
<b>Initialization</b>	
Methods	Hybrid

### 3. Results and Discussion

Prior to conducting any scientific or engineering investigation, including the examination of turbulence kinetic energy, it is crucial to validate the data. Data validation involves assessing the standards, accuracy, and reliability of the information collected or obtained for a particular study or experiment. Validating the data ensures that it is trustworthy and suitable for the intended purpose, thereby enhancing confidence in the study's findings and interpretations.

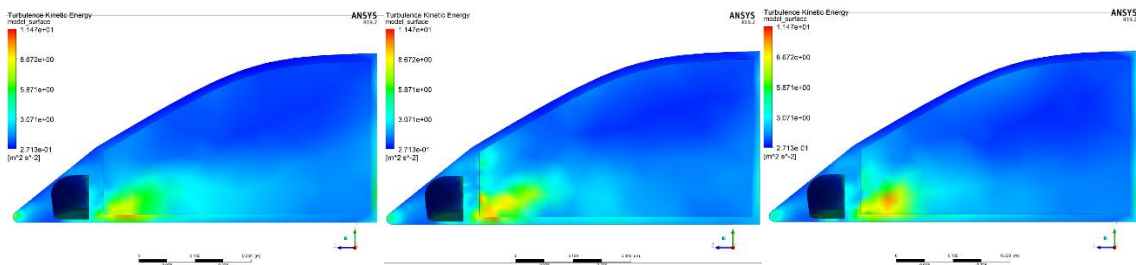


**Figure 5: Turbulence Kinetic Energy Contour act on Door Mirror with 3 Different Condition at speed 50km/h**

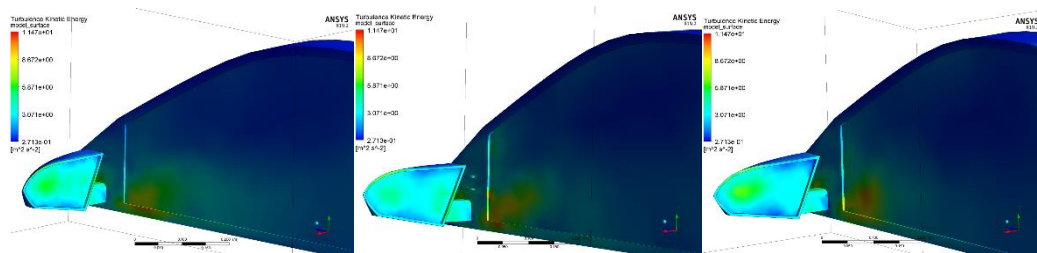


**Figure 6: Turbulence Kinetic Energy Contour act on Side Mirror with 3 Different Condition at speed 50km/h**

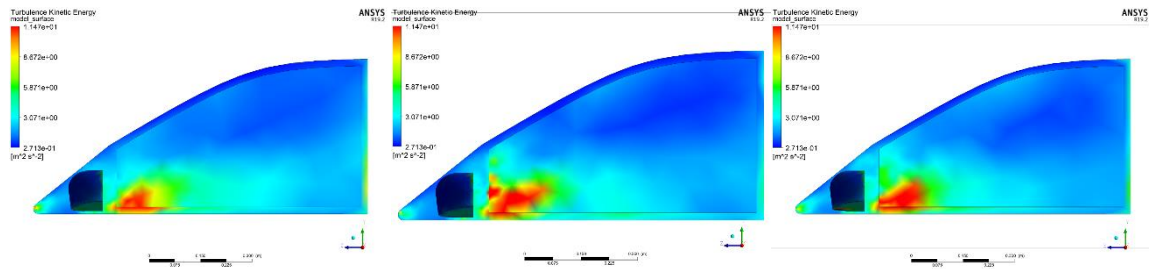


**Figure 7: Turbulence Kinetic Energy Contour act on Door Mirror with 3 Different Condition at speed 60km/h**

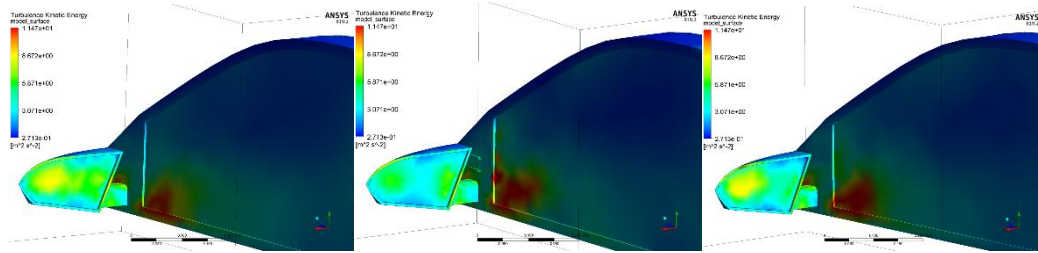


**Figure 8: Turbulence Kinetic Energy Contour act on Side Mirror with 3 Different Condition at speed 60km/h**

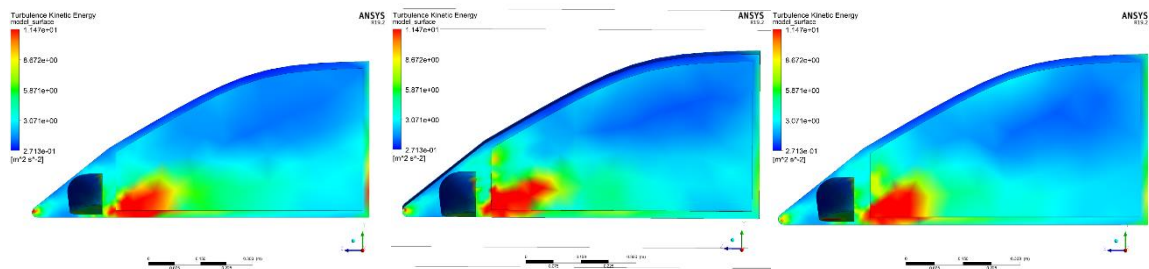


**Figure 9: Turbulence Kinetic Energy Contour act on Door Mirror with 3 Different Condition at speed 70km/h**

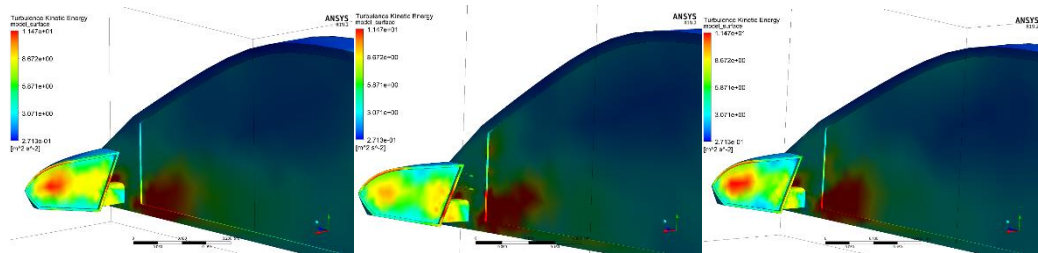


**Figure 10: Turbulence Kinetic Energy Contour act on Side Mirror with 3 Different Condition at speed 70km/h**

Based on Figure 5,6,7,8,9 and 10, shows the CFD analysis result of the turbulence kinetic energy contour act on 3 different conditions at door mirror and side mirror at speed 50km/h, 60km/h, and 70km/h. The 3 different conditions are the model without any additional shark fin, model with additional shark fin at base of side mirror and model with additional shark fin at side mirror. Based on figure 5,7 and 9, the area least affected by turbulence kinetic energy act on door mirror can be observed in the model without any extra shark fin, either on the base or on the side mirror. On the other hand, the model with an additional shark fin at the base of the side mirror is the most adversely affected by turbulence kinetic energy. This is due to the alteration of airflow patterns around the side mirror caused by the presence of fins. Based on Figure 6,8 and 10, the area least affected by turbulence kinetic energy can be observed in the model equipped with a shark fin on the side mirror. Conversely, the model without

any additional shark fin is the most adversely affected by turbulence kinetic energy. This is because the presence of fins can alter the airflow patterns around the side mirror. The shark fin positioned on the outside rearview mirror assists in reducing the accumulation of airflow on the surface area of the mirror [9].

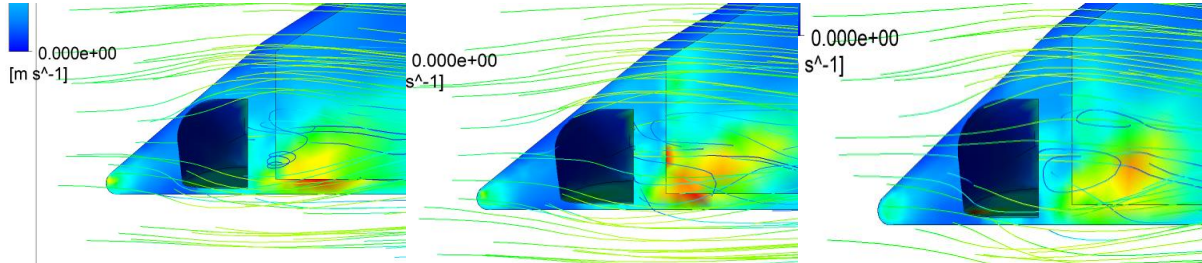


**Figure 11: Turbulence Kinetic Energy Streamline act on Door Mirror with 3 Different Condition at speed 50km/h**

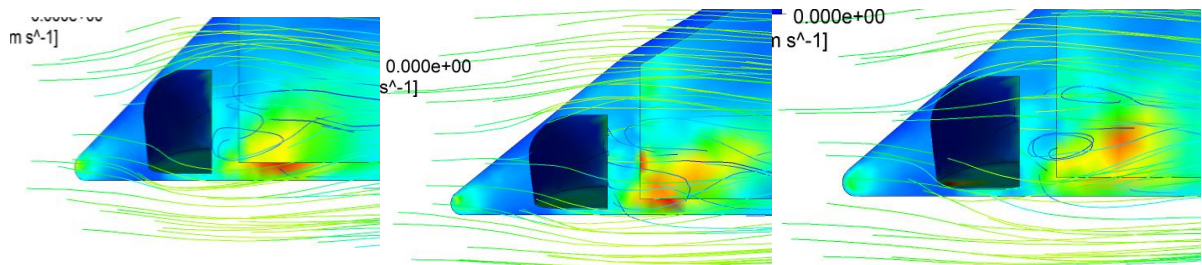


**Figure 12: Turbulence Kinetic Energy Streamline act on Door Mirror with 3 Different Condition at speed 60km/h**

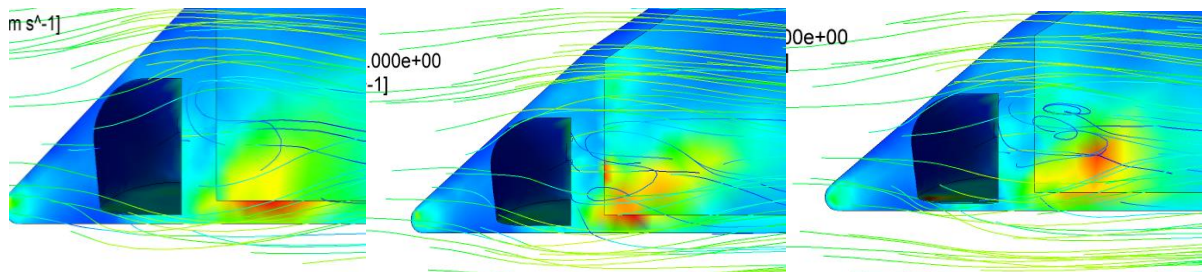


**Figure 13: Turbulence Kinetic Energy Streamline act on Door Mirror with 3 Different Condition at speed 70km/h**

Based on Figure 11,12 and 13, it is evident that the streamline exhibits turbulence effects after passing through the side mirror. Among the models examined, the one with additional shark fin at side mirror base demonstrates the most significant turbulence effect on the streamline, while the model equipped with an additional shark fin on the side mirror base the least turbulence effect. This phenomenon occurs due to the wake region formed behind the side mirror, where the flow of fluid, typically air, encounters disruptions and undergoes a transition into a turbulent state. The presence of the mirror acts as an obstacle, disturbing the smooth flow of the fluid and causing changes in velocity, pressure, and flow characteristics.

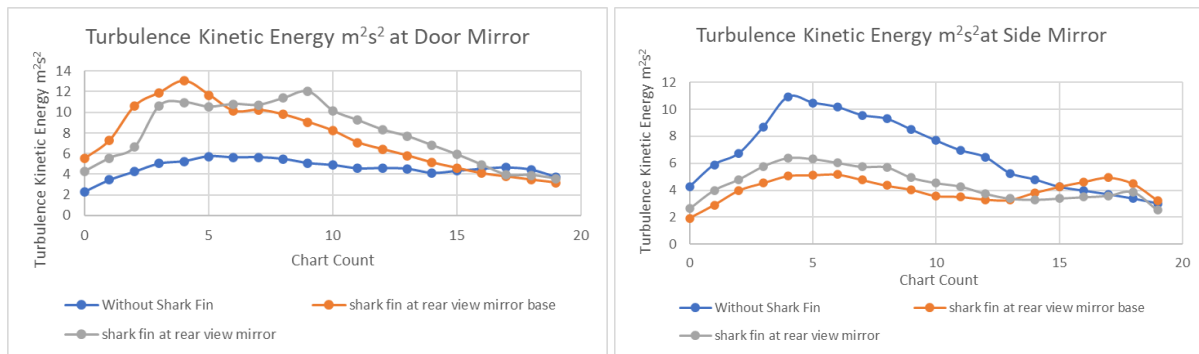


**Figure 14: Turbulence Kinetic Energy Graph vs Chart Count at Door Mirror and side mirror at speed 50km/h**

The provided graph displays the turbulence kinetic energy acting on the side mirror and door mirror for three different model simulations, one without a shark fin, one with an additional shark fin at the base of the side mirror, and one with an additional shark fin at the side mirror. Among these models, the model with an additional shark fin at the side mirror base exhibits the highest turbulence kinetic energy, reaching its peak at the fourth data point on the chart with a value of 13.04 m<sup>2</sup>s<sup>-2</sup>. In comparison, the other models have lower turbulence kinetic energy values. Following the peak, the turbulence kinetic energy experiences a significant decrease until the end of the data. This decline is a result of energy dissipation, which occurs as the energy cascades to smaller scales within the turbulent flow. At the beginning of the data, the model without a shark fin demonstrates the lowest turbulence kinetic energy, measuring at 5.73 m<sup>2</sup>s<sup>-2</sup>. Meanwhile the side mirror model without shark fin has the highest amount of turbulence kinetic energy while the model with shark fin at base side mirror has the lowest turbulence kinetic energy effect on side mirror graph.

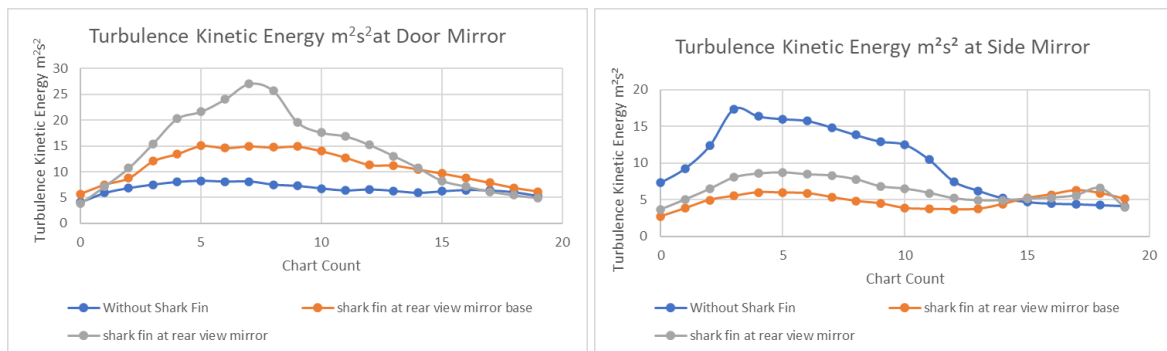


**Figure 15: Turbulence Kinetic Energy Graph vs Chart Count at Door Mirror and side mirror at speed 60km/h**

The provided graph displays the turbulence kinetic energy acting on the side mirror and door mirror for three different model simulations, one without a shark fin, one with an additional shark fin at the base of the side mirror, and one with an additional shark fin at the side mirror. Among these models, the model with an additional shark fin at the side mirror exhibits the highest turbulence kinetic energy, reaching its peak at the fourth data point on the chart with a value of 27.05 m<sup>2</sup>s<sup>-2</sup>. In comparison, the other models have lower turbulence kinetic energy values. Following the peak, the turbulence kinetic energy experiences a significant decrease until the end of the data. This decline is a result of energy dissipation, which occurs as the energy cascades to smaller scales within the turbulent flow. At the beginning of the data, the model without a shark fin demonstrates the lowest turbulence kinetic energy, measuring at 3.79 m<sup>2</sup>s<sup>-2</sup>. Meanwhile the side mirror model without shark fin has the highest amount of



turbulence kinetic energy while the model with shark fin at side mirror has the lowest turbulence kinetic energy effect on side mirror graph.

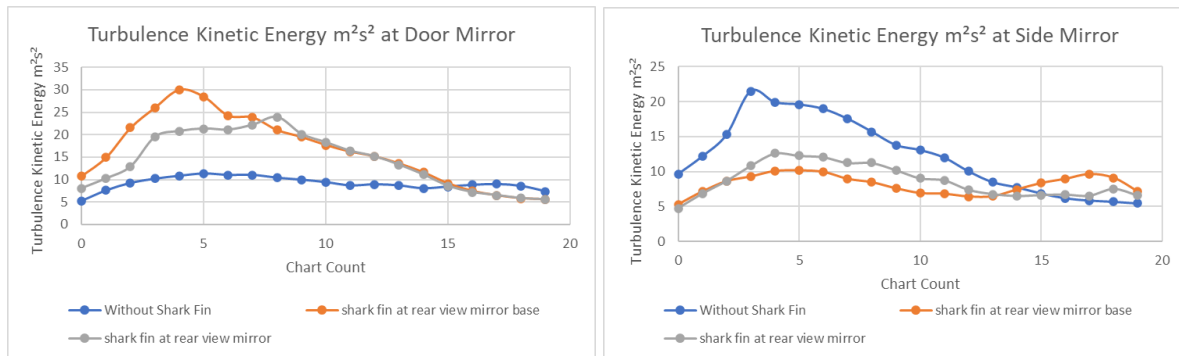


**Figure 16: Turbulence Kinetic Energy Graph vs Chart Count at Door Mirror and side mirror at speed 70km/h**

The provided graph displays the turbulence kinetic energy acting on the side mirror and door mirror for three different model simulations, one without a shark fin, one with an additional shark fin at the base of the side mirror, and one with an additional shark fin at the side mirror. Among these models, the model with an additional shark fin at the side mirror base exhibits the highest turbulence kinetic energy, reaching its peak at the fourth data point on the chart with a value of  $30.05 \text{ m}^2\text{s}^{-2}$ . In comparison, the other models have lower turbulence kinetic energy values. Following the peak, the turbulence kinetic energy experiences a significant decrease until the end of the data. This decline is a result of energy dissipation, which occurs as the energy cascades to smaller scales within the turbulent flow. At the beginning of the data, the model without a shark fin demonstrates the lowest turbulence kinetic energy, measuring at  $5.24 \text{ m}^2\text{s}^{-2}$ . Meanwhile the side mirror model without shark fin has the highest amount of turbulence kinetic energy while the model with shark fin at side mirror has the lowest turbulence kinetic energy effect on side mirror graph.

#### 4. Conclusion

Based on the simulation results, it was observed that the model without a shark fin exhibited better performance in terms of turbulence kinetic energy on the door mirror. This model experienced lower turbulence kinetic energy, indicating reduced flow disturbances and improved aerodynamics. However, it had the worst result in terms of turbulence kinetic energy on the outside rear view mirror. On the other hand, the model with an additional shark fin at the base of the outside rear view mirror showed the best results in terms of turbulence kinetic energy. It demonstrated the lowest amount of turbulence kinetic energy acting on the outside rear view mirror, indicating improved airflow and reduced flow disruptions. This model showcased an enhancement in turbulence kinetic energy compared to the model without any additional shark fin. Therefore, it can be concluded that the addition of a shark fin, particularly at the base of the outside rear view mirror, can contribute to the reduction of turbulence kinetic energy and improve aerodynamic performance in terms of water deposition.

#### Acknowledgement

The authors would also like to thank the Faculty of Engineering Technology, Universiti Tun Hussein Onn Malaysia for its support.

## References

- [1] Hucho, W.-H., & Sovran, G. (1993). Aerodynamic of Road Vehicles. In *Annu. Rev. Fluid Mech* (Vol. 25). [www.annualreviews.org](http://www.annualreviews.org)
- [2] Larchez, A., & Naghdy, F. (2005). Real time prediction of vehicle mirror vibration Real time prediction of vehicle mirror vibration Real Time Prediction of Vehicle Mirror Vibration. <https://ro.uow.edu.au/engpapershttps://ro.uow.edu.au/engpapers/589https://ro.uow.edu.au/engpapers/589>
- [3] Gaylard, A. P., Kirwan, K., & Lockerby, D. A. (2017). Surface contamination of cars: A review. *Proceedings of the Institution of Mechanical Engineers, Part D: Journal of Automobile Engineering*, 231(9), 1160–1176. <https://doi.org/10.1177/0954407017695141>
- [4] Bannister, M. (2018). Drag and Dirt Deposition Mechanisms of External Rear View Mirrors and Techniques Used for Optimisation.
- [5] Ayres, T., Li, L., Trachtman, D., & Young, D. (2005). Passenger-side rear-view mirrors: driver behavior and safety. *International Journal of Industrial Ergonomics*, 35(2), 157–162. <https://doi.org/10.1016/j.ergon.2004.05.009>
- [6] Zaareer, M., & Mourad, A.-H. (2022). Effect of Vehicle Side Mirror Base Position on Aerodynamic Forces and Acoustics. *Alexandria Engineering Journal*, 61(2), 1437–1448. <https://doi.org/10.1016/j.aej.2021.06.049>
- [7] Ye, J., Xu, M., Xing, P., Cheng, Y., Meng, D., Tang, Y., & Zhu, M. (2021). Investigation of aerodynamic noise reduction of exterior side view mirror based on bionic shark fin structure. *Applied Acoustics*, 182, 108188. <https://doi.org/10.1016/j.apacoust.2021.108188>
- [8] Chu Y, Shin Y, Lee S. (2018). Aerodynamic Analysis and Noise-Reducing Design of an Outside Rear View Mirror. . *Applied Sciences Journal*, 8(4), 519
- [9] Fox, Rodney O. (2021). Multiphase Turbulence. *Advanced Approaches in Turbulence*, 307–371.